ACS Infectious Diseases

pubs.acs.org/journal/aidcbc
Article

Integrated Transcriptomic and Metabolomic Mapping Reveals the Mechanism of Action of Ceftazidime/Avibactam against Pan-Drug-Resistant *Klebsiella pneumoniae*

Maytham Hussein, Rafah Allobawi, Jinxin Zhao, Heidi Yu, Stephanie L. Neville, Jonathan Wilksch, Labell J. M. Wong, Mark Baker, Christopher A. McDevitt, Gauri G. Rao, Jian Li,* and Tony Velkov*

Cite This: *ACS Infect. Dis.* 2023, 9, 2409−2422
Read Online

ACCESS | Metrics & More | Article Recommendations | Supporting Information

ABSTRACT: Here, we employed an integrated metabolomics and transcriptomics approach to investigate the molecular mechanism(s) of action of ceftazidime/avibactam against a pan-drug-resistant *K. pneumoniae* clinical isolate from a patient with urinary tract infection. Ceftazidime/avibactam induced time-dependent perturbations in the metabolome and transcriptome of the bacterium, mainly at 6 h, with minimal effects at 1 and 3 h. Metabolomics analysis revealed a notable reduction in essential lipids involved in outer membrane glycerolipid biogenesis. This disruption effect extended to peptidoglycan and lipopolysaccharide biosynthetic pathways, including lipid A and *O*-antigen assembly. Importantly, ceftazidime/avibactam not only affected the final steps of peptidoglycan biosynthesis in the periplasm, a common mechanism of ceftazidime action, but also influenced the synthesis of lipid-linked intermediates and early stages of cytoplasmic peptidoglycan synthesis. Furthermore, ceftazidime/avibactam substantially inhibited central carbon metabolism (e.g., the pentose phosphate pathway and tricarboxylic acid cycle). Consistently, the dysregulation of genes governing these metabolic pathways aligned with the metabolomics findings. Certain metabolomics and transcriptomics signatures associated with ceftazidime resistance were also perturbed. Consistent with the primary target of antibiotic activity, biochemical assays also confirmed the direct impact of ceftazidime/avibactam on peptidoglycan production. This study explored the intricate interactions of ceftazidime and avibactam within bacterial cells, including their impact on cell envelope biogenesis and central carbon metabolism. Our findings revealed the complexities of how ceftazidime/avibactam operates, such as hindering peptidoglycan formation in different cellular compartments. In summary, this study confirms the existing hypotheses about the antibacterial and resistance mechanisms of ceftazidime/avibactam while uncovering novel insights, including its impact on lipopolysaccharide formation.

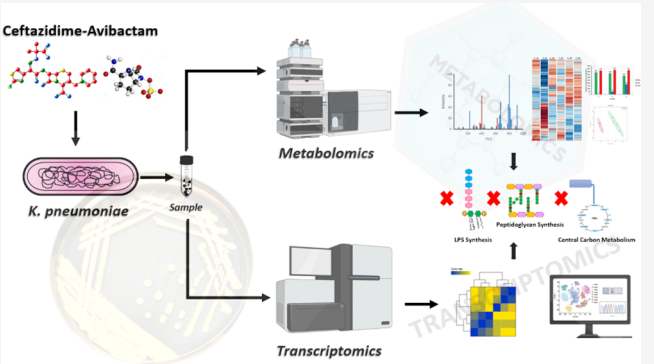

KEYWORDS: *ceftazidime-avibactam, K. pneumoniae, antimicrobial resistance, metabolomics, transcriptomics*

The World Health Organization (WHO) has highlighted antimicrobial resistance (AMR) as one of the top ten greatest threats to human health.[1] *Klebsiella pneumoniae*, a Gram-negative human pathogen responsible for various nosocomial infections, including urinary tract infections (UTIs) and pneumonia, was responsible for 9.9% of all hospital-acquired infections in the United States in 2014.[2] Historically, these infections were treated with β-lactams antibiotics, but the emergence of multidrug-resistant (MDR) *K. pneumoniae* has rendered many conventional therapies ineffective.[3,4] One study reported that the crude mortality rate of a population infected with carbapenem-resistant *K. pneumoniae* was a staggering 71.9%.[5] An existing strategy to treat pan-drug-resistant (PDR) pathogens is through antibiotic/adjuvant combinations such as the β-lactam/β-lactamase inhibitor combination ceftazidime/avibactam (Avycaz).[6]

Ceftazidime/avibactam is a third-generation cephalosporin β-lactam combined with avibactam, a novel expanded-spectrum β-lactamase inhibitor.[7,8] This combination therapy was approved in 2015 for the treatment of complicated intra-abdominal infections, UTIs, and pneumonia.[9] Not unlike other β-lactams, ceftazidime primarily exerts its antibacterial activity by binding to penicillin-binding proteins, thereby inhibiting the cross-linking of peptidoglycan during cell wall synthesis,

Received: June 5, 2023
Revised: October 2, 2023
Accepted: October 11, 2023
Published: October 25, 2023

Table 1. Significantly Perturbed Lipids in the *K. pneumoniae* FADDI-KP070 Metabolome Following Treatment with Ceftazidime/Avibactam (log_2 FC $\geq$ 0.59 or $\leq$ −0.59, p < 0.05)

lipid intermediates				log_2FC		
lipid	class	formula	mass	1 h	3 h	6 h
palmitic acid	lipid	C16H32O2	256.4			3.26
phosphatidic acid	lipid	C5H7O8PR2	226.07			−2.76
tetradecanoic acid	lipid	C14H28O2	228.20			2.03
(R)-3-hydroxybutanoate	lipid	C4H8O3	104.04			−1.00
(9Z)-hexadecenoic acid	lipid	C16H30O2	254.22			4.26
sn-glycerol 3-phosphate	lipid	C3H9O6P	172.01			6.18
heptaprenyl diphosphate	lipid	C35H60O7P2	654.38		−2.80	−2.91
FA (12:1)	FAs	C12H24O	184.18			−1.98
FA (20:4)	FAs	C20H32O2	304.24			−3.40
FA oxo(5:0)	FAs	C5H8O3	116.04			−3.32
2-butenoate	FAs	C4H6O2	86.036			−4.76
FA hydroxy(4:0)	FAs	C8H13NO4	187.08			−3.38
FA hydroxy(6:0)	FAs	C6H12O3	132.07			−3.42
FA hydroxy(9:0)	FAs	C9H18O3	174.12			1.34
FA methyl(16:1)	FAs	C17H32O2	268.24			6.78
5-hydroxypentanoate	FAs	C5H10O3	118.06			−3.81
formyl-3-hydroxybutanoate	FAs	C5H10O3	118.06			−3.16
2-amino-4-methylpentanoic	FAs	C6H13NO2	131.09			−1.99
2-C-methyl-D-erythritol-4P	FAs	C5H13O7P	216.04			−3.18
PS(18:1)	GPLs	C24H46NO9P	523.29		−2.14	−5.49
PS(18:0)	GPLs	C24H48NO9P	525.30			−5.41
PI(33:2)	GPLs	C42H77O13P	842.48			−5.11
PI(18:2)	GPLs	C27H49O12P	596.29			−4.73
PI(18:1)	GPLs	C27H51O12P	598.31			−4.64
PI(16:0)	GPLs	C25H49O12P	572.29			−4.51
PG(35:1)	GPLs	C41H79O10P	762.54			−5.84
PG(37:2)	GPLs	C43H81O10P	788.55			−3.93
PG(36:2)	GPLs	C42H79O10P	774.54			−3.91
PG(35:2)	GPLs	C41H77O10P	760.52			−3.79
PG(34:2)	GPLs	C40H75O10P	746.51			−3.78
PG(34:1)	GPLs	C40H77O10P	748.52			−3.74
PG(33:1)	GPLs	C39H75O10P	734.50			−3.71
PG(32:2)	GPLs	C38H71O10P	718.47			−3.59
PG(32:1)	GPLs	C38H73O10P	720.49			−3.38
PG(31:1)	GPLs	C37H71O10P	706.47			−3.34
PG(30:1)	GPLs	C36H69O10P	692.46			−3.32
PG(30:0)	GPLs	C36H71O10P	694.47			−3.32
PG(19:1(9Z)/0:0)	GPLs	C25H49O9P	524.31			−3.19
PG(17:1)	GPLs	C23H45O9P	496.28			−2.96
PG (28:0)	GPLs	C34H67O10P	666.44			−2.91
PG (16:0)	GPLs	C22H45O9P	484.28			−2.87
PE(36:2)	GPLs	C41H78NO8P	743.54		−1.50	−2.84
PE(34:1)	GPLs	C39H76NO8P	717.53			−2.83
PE(30:1)	GPLs	C35H68NO8P	661.46		−2.06	−2.75
PE(30:0)	GPLs	C35H70NO8P	663.48			−2.70
PE(28:0)	GPLs	C33H66NO8P	635.45			−2.69
PC(6:2)	GPLs	C14H32NO6P	341.19			−2.53
PC(32:2)	GPLs	C40H76NO8P	729.53			−2.51
PC(32:1)	GPLs	C40H78NO8P	731.54			−2.51
PC(30:1)	GPLs	C38H74NO8P	703.51			−2.41
PA(30:1)	GPLs	C33H63O8P	618.42			−2.38
PA(30:0)	GPLs	C33H65O8P	620.44			−2.11
PA(16:0/0:0)	GPLs	C19H39O7P	410.24			−1.96
PA(14:0/0:0)	GPLs	C17H35O7P	382.21			−0.94
lysoPE(18:2)	GPLs	C23H44NO7P	477.28			−0.87
lysoPE(18:0)	GPLs	C23H48NO7P	481.31			1.05
lysoPE(0:0/14:0)	GPLs	C19H40NO7P	425.25			1.45
lysoPC(16:1(9Z))	GPLs	C24H48NO7P	493.31		1.64	1.90

https://doi.org/10.1021/acsinfecdis.3c00264
ACS Infect. Dis. 2023, 9, 2409−2422

Table 1. continued

lipid intermediates				log_2FC		
lipid	class	formula	mass	1 h	3 h	6 h
lysoPC(16:0)	GPLs	C24H50NO7P	495.33		4.10	2.27
lysoPC(14:1)	GPLs	C22H44NO7P	465.28			2.47

FAs, fatty acids; GPLs, glycerophospholipids; PE, phosphoethanolamines; PG, glycerophosphoglycerols; PS, glycerophosphoserines; PC, glycerophosphocholines; PA, glycerophosphates; PI, glycerophosphoinositols; LysoPE, lysophosphatidylethanolamines; and lysoPC, lysophosphatidylcholines.

ultimately leading to bacterial cell lysis.[10] The second component of the formulation, avibactam (a non-β-lactam β-lactamase inhibitor) plays a crucial role in preserving ceftazidime's activity by inhibiting class A, C, and D β-lactamases, albeit, it is not active against class B β-lactamases, such as New Delhi metallo-β-lactamase (NDM) and Verona integron-encoded (VIM).[6] Notably, avibactam, at concentrations ≥8 mg/L, has low intrinsic antimicrobial activity against some Enterobacteriaceae, including *E. coli* and *K. pneumoniae*.[11]

Ceftazidime/avibactam has been used over the past few years as a salvage treatment for KPC-positive *K. pneumoniae* infections and it is classed as a reserve antibiotic under the WHO's AWaRe (Access, Watch, and Reserve) scheme for the treatment of PDR infections.[12] Worryingly, several hospitals across Europe and China have now reported the emergence of ceftazidime/avibactam-resistant *K. pneumoniae* isolates, including KPC-2 and KPC-3-producing strains.[13−15] This concerning trend highlights the importance of developing our understanding of the precise mechanism(s) of action of ceftazidime/avibactam at the molecular level. Most, if not all, antibiotics have multiple targets or at least multiple effects, i.e., more than one mechanism of action, motivating the thorough exploration of multitarget approaches to combat resistant bacteria.[16] Over the past decade, advanced high-throughput sequencing has allowed deeper interrogation of the cellular impact of anti-infectives against bacteria. Employing "omics" studies, such as metabolomics and transcriptomics, alongside computational techniques can provide a system-level overview of the molecular interactions between drugs and their targets.[17−21]

The objective of this study was to elucidate the molecular mechanism(s) of the antibacterial synergy of ceftazidime/avibactam against PDR *K. pneumoniae* using an integrated metabolomics and transcriptomics approach. Our analyses reveal a much broader set of mechanism(s) of action of ceftazidime/avibactam beyond the central dogma of inhibition of cell wall biosynthesis.

RESULTS AND DISCUSSION

Metabolomics Analysis. The minimum inhibitory concentration (MIC) of ceftazidime/avibactam and an antibiogram profile for the PDR *K. pneumoniae* FADDI-KP070 (ceftazidime/avibactam MIC = 8/4 mg/L) isolated from a patient with a UTI are presented in Table S1. A static time-kill assay was performed to assess various ceftazidime/avibactam concentrations: 1 × MIC (mg/L): 8/4; 2 × MIC (mg/L): 16/4; 4 × MIC (mg/L): 32/4; 6 × MIC (mg/L): 48/4; 8 × MIC (mg/L): 64/4. This assay targeted *K. pneumoniae* FADDI-KP070 during late-exponential-phase growth (~10^8 CFU/mL) at different time points (1, 3, and 6 h). The aim was to get optimal conditions for metabolomic sampling while avoiding extensive bacterial killing (Figure S1).[22−25] Based on the results, a concentration of 48/4 mg/L, equivalent to 6 x MIC of ceftazidime/avibactam, was selected as an optimal concentration for the subsequent metabolomics study.

Metabolomics data profiling and annotation identified 1569 putative metabolites across all time points (1, 3, and 6 h). It is important to note that not all of these metabolites displayed alterations; rather, this number represents the comprehensive set of identified metabolites. Undefined metabolites (n = 452), peptides (n = 358), amino acids (n = 276), and lipids (n = 214) formed the majority of metabolite classes, followed by carbohydrates (n = 100), nucleotides (n = 70), cofactors and vitamins (n = 55), secondary metabolites (n = 27), and the least abundant class was metabolites involved in energy metabolism (n = 17) (Figure S2).

To understand the data further, multivariate and univariate analyses statistics (log_2-fold change [FC] ≥ 0.59 or ≤−0.59, corresponding to a metabolite level change of approximately 1.5-fold; $p < 0.05$) were used to identify clusters and significant metabolites affected at 1, 3, and 6 h post ceftazidime/avibactam treatment. PCA plots revealed that the ceftazidime/avibactam treated samples were clustered together with the untreated control at 1 and 3 h but separated from the untreated control at 6 h (Figure S3A). This observation was consistent with the heat maps, which also showed that ceftazidime/avibactam treatment induced extensive perturbations predominantly at 6 h (Figure S3B). Consistent with this observation, the volcano plots revealed the greatest perturbations in response to ceftazidime/avibactam treatment were at the 6 h time point, with 558 (352 decreased and 206 increased) metabolites perturbed (Figure S4A) compared with only 34 (13 decreased and 21 increased) and 14 (5 decreased and 9 increased) significantly perturbed metabolites at 1 and 3 h, respectively (Figure S4A). Metabolic profiling analysis showed that at 6 h ceftazidime/avibactam treatment largely perturbed peptides (mainly increased), amino acids, and lipids (mainly decreased) and slightly impacted carbohydrate, nucleotide, energy, cofactor, and vitamin metabolism (Figure S4B). Notably, 6 (1 h), 9 (3 h), and 533 (6 h) uniquely altered metabolites were detected, of which only two (anthranilate and 1,6-anhydro-*N*-acetylmuramate) were common across all exposure times (Figure S4C).

Transcriptomics Analysis. We next performed a transcriptomics study on the same bacterial culture used for the metabolomics analysis. Consistent with the metabolomics data, PCA graphs revealed a significant gap between the ceftazidime/avibactam samples at 6 h and the untreated control, while the 1 and 3 h samples were clustered closer to the untreated control (Figure S5A). The dramatic changes (log_2-fold change [FC] ≥ 0.59 or ≤ −0.59, corresponding to a transcript level change of approximately 1.5-fold, false discovery rate (FDR) < 0.05) in gene expression in the *K. pneumoniae* FADDI-KP070 transcriptome occurring at 6 h were characterized by induction of 909/858 (up/down) differentially expressed genes (DEGs) (Figure S5B) compared

https://doi.org/10.1021/acsinfecdis.3c00264
ACS Infect. Dis. 2023, 9, 2409−2422

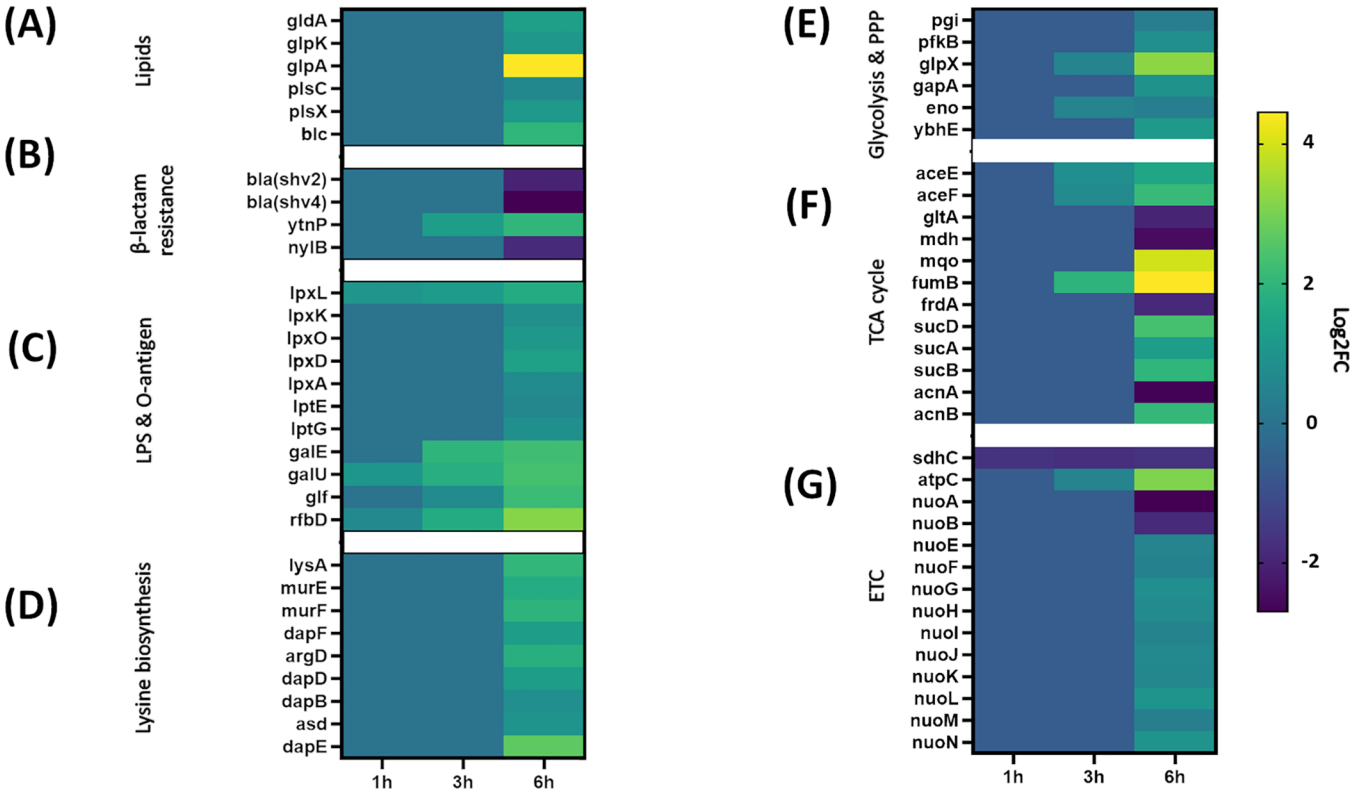

Figure 1. Comparative transcriptome mapping revealed differentially expressed genes (log_2-fold change) of PDR *K. pneumoniae* FADD-KP070 in response to treatment with ceftazidime/avibactam (48/4 mg/L). Major DEGs detected at 1, 3, and 6 h ($log_2FC \geq 0.59$ or ≤ -0.59, false discovery rate (FDR) < 0.05) were involved in the biosynthesis of (A) bacterial membrane lipids, (B) *β*-lactam resistance, (C) cell envelope pathways [lipopolysaccharide (LPS), *O*-antigen assembly], (D) lysine biosynthesis and central carbon metabolism, (E) glycolysis and pentose phosphate pathway (PPP), (F) tricarboxylic acid (TCA) cycle, and (G) electron transport chain (ETC).

with 127 (110 up/17 down) and 477 (281 up/166 down) DEGs at 1 and 3 h, respectively (Figure S5B). Of note, 9 (1 h), 113 (3 h), and 1423 (6 h) DEGs were uniquely altered at each exposure time (Figure S5C). Venn diagrams generated from the RNA expression profiles also revealed that there were 94 common DEGs between all time points (1, 3, and 6 h) (Figure S5C).

A similar pattern to the metabolomics analysis was obtained following mapping of DEGs across 1, 3, and 6 h, with pathways related to cell envelope biogenesis, central carbon metabolism, and fatty acid biosynthesis all significantly impacted. The gene names and annotations of the DEGs are documented in Table S2.

Correlative Metabolic and Transcriptomic Analyses of Perturbations in Lipid Metabolism. Notably, ceftazidime/avibactam treatment had no impact on lipid intermediates of *K. pneumoniae* FADDI-KP070 at 1h, with only slight effects at 3 h. However, significant perturbations became evident after 6 h (Table 1). At 3 h, only six lipid intermediates (including five glycerophospholipids and heptaprenyl diphosphate) were significantly perturbed in response to ceftazidime/avibactam treatment ($log_2FC > 1.0$, $p < 0.05$; Table 1). By comparison, there were extensive changes in the abundance of various bacterial membrane lipids, glycerophospholipids (GLPs), and fatty acids (FAs) at 6 h ($log_2FC > 1.0$, $p < 0.05$; Table 1). Notably, ceftazidime/avibactam perturbed GLPs (largely decreased), followed by FAs (mainly decreased). Other perturbed lipids were phosphatidic acid (PtdOH, $log_2FC = -2.76$), palmitic acid ($log_2FC = 3.26$), tetradecanoic acid ($log_2FC = 2.03$), and *sn*-glycerol 3-phosphate ($log_2FC = 6.18$), the main intermediates involved in the biogenesis of outer membrane glycerolipids.[22,26] Although Gram-negative bacteria employ an array of phospholipid headgroup structures in their outer membrane, the common element across all head groups is PtdOH, for which *sn*-glycerol 3-phosphate is the universal source of the glycerol backbone. The central importance of PtdOH recycling and formation in bacterial physiology suggests that these pathways are potentially ideal targets for the development of new antibacterial therapeutics.[27,28] Importantly, the abundance of heptaprenyl diphosphate, a lipid that governs the formation of menaquinone, a key electron transporter in bacteria, significantly decreased in response to ceftazidime/avibactam treatment ($log_2FC = -2.80$; Table 1). Notably, inhibition of heptaprenyl diphosphate synthase has been reported to impact the bactericidal activity, again highlighting the importance of this key intermediate for bacterial survival.[29,30] Consistent with our findings, a previous metabolomics study that investigated the mechanisms of ceftazidime resistance in the Gram-negative *Vibrio alginolyticus* reported that dysregulated fatty acid biosynthesis and increase in some biomarkers (e.g., palmitic acid and stearic acid) were the key metabolic biomarkers associated with resistance.[31]

Consistent with the metabolomics data, transcriptomics analysis at 6 h showed a significant dysregulation in the expression of genes involved in bacterial glycerolipid biosynthesis, including *gldA*, *glpK*, *glpA*, *plsX* and *plsC* ($log_2FC > 1.0$, FDR < 0.05; Figure 1A).

This phenomenon has also been reported as a mechanism of antibacterial activity for agents from other antibiotic

https://doi.org/10.1021/acsinfecdis.3c00264
ACS Infect. Dis. 2023, 9, 2409−2422

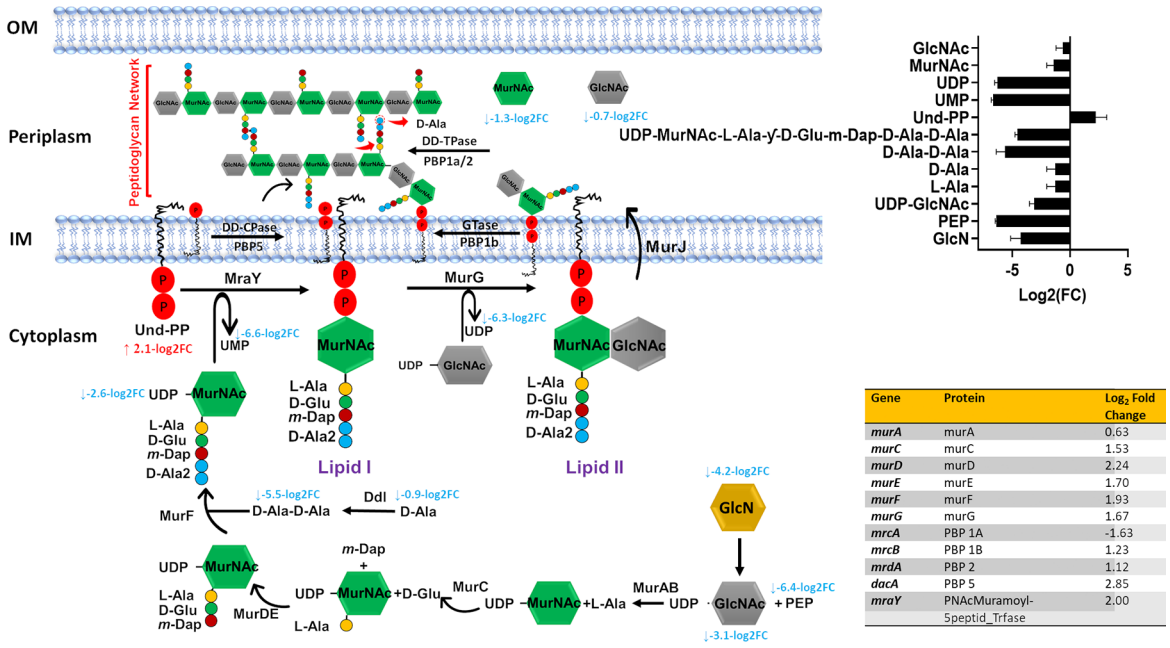

Gene	Protein	Log_2 Fold Change
murA	murA	0.63
murC	murC	1.53
murD	murD	2.24
murE	murE	1.70
murF	murF	1.93
murG	murG	1.67
mrcA	PBP 1A	-1.63
mrcB	PBP 1B	1.23
mrdA	PBP 2	1.12
dacA	PBP 5	2.85
mraY	PNAcMuramoyl-5peptid_Trfase	2.00

Figure 2. Schematic pathway diagram showing the three stages of peptidoglycan biosynthesis (cytoplasmic precursor synthesis, membrane translocation, and polymerization and cross-linking) impacted by ceftazidime/avibactam treatment (48/4 mg/L) at 6 h. The diagram also shows the bar charts and table for the significantly impacted metabolites and genes involved in this metabolic pathway, respectively ($log_2FC \geq 0.59$ or ≤ -0.59, $p < 0.05$, false discovery rate (FDR) < 0.05).

classes.[32,33] Overexpression of *plsC*, encoding 1-acyl-*sn*-glycerol-3-phosphate acyltransferase, an enzyme that mediates the conversion of 1-acyl-*sn*-glycerol-3-phosphate to phosphatidic acid, has been found to play a critical role in tigecycline resistance in *Acinetobacter baumannii*.[32] Similarly, mupirocin and other FASII agents that inhibit fatty acid biosynthesis were found to inhibit the phospholipid biosynthetic genes *plsX* and *plsC*.[33]

Metabolic and Transcriptomic Changes in Cell Envelope Biogenesis. *Peptidoglycan Biosynthesis.* It is well established that β-lactam antibiotics such as ceftazidime primarily exert their antibacterial action by inhibition of peptidoglycan biosynthesis in the bacterial cell wall.[34] This antibacterial effect is primarily achieved by inhibiting enzymes such as penicillin-binding proteins 1 and 3 (PBP1 and PBP3). These enzymes are responsible for peptidoglycan formation by catalyzing the polymerization of the glycan strand (transglycosylation) and cross-linking of glycan chains (transpeptidation).[6,35] Concordant with this bactericidal action, metabolomics data analysis at 6 h revealed that ceftazidime/avibactam significantly reduced the abundance of two essential amino sugars, namely, *N*-acetylmuramic acid [MurNAc] and *N*-acetyl-D-glucosamine [GlcNAc] ($log_2FC > -0.59$, $p < 0.05$; Figure 2).

These two monosaccharides are both derived from UDP-GlcNAc and linked β-(1,4) alternatively (transglycosylation) to form the mature peptidoglycan network.[36,37] Notably, the abundance of UDP-*N*-acetyl-D-glucosamine [UDP-GlcNAc] ($log_2FC = -3.10$) and D-alanine [D-Ala] ($log_2FC = -0.90$) also declined 6 h after ceftazidime/avibactam treatment, suggesting that ceftazidime/avibactam primarily interferes with the final steps of peptidoglycan production (transglycosylation and transpeptidation) (Figure 2).

The transcriptomics results were consistent with the metabolomics analysis, with a significant perturbation in transcription of genes *mrcA/B*, *mrdA* and *dacA*, governing the key penicillin-binding proteins PBP 1A/1B, PBP 2, and PBP 5, respectively ($log_2FC > 1.0$, FDR < 0.05; Figure 2). These proteins are primarily responsible for peptidoglycan transpeptidations such as the removal of the terminal D-alanine by PBP 1A (Figure 2).[38]

The initial steps of peptidoglycan synthesis occur inside the cytoplasm and include the synthesis of the nucleotide precursors and assembly of the peptide stem, leading to the formation of UDP-MurNAc-pentapeptide (UDP-*N*-acetylmuramoyl-L-alanyl-D-glutamyl-6-carboxy-L-lysyl-D-alanyl- D-alanine).[39] This process is mediated by a series of essential enzymes, known as the Mur ligases MurA, B, C, D, E, and F encoded by *murABCDEF*.[40] Intriguingly, ceftazidime/avibactam significantly perturbed the abundance of principal elements involved in the early cytoplasmic stages of peptidoglycan biogenesis at 6 h, including phosphoenolpyruvate [PEP], D-glucosamine [GlcN], UDP-*N*-acetyl-D-glucosamine [UDP-GlcNAc], L-alanine [L-Ala], D-alanyl-D-alanine [D-Ala-D-Ala], and UDP-*N*-acetylmuramoyl-L-alanyl-D-glutamyl-6-carboxy-L-lysyl-D-alanyl-D-alanine[UDP-MurNAc-L-Ala-γ-D-Glu-m-Dap-D-Ala-D-Ala] ($log_2FC > -2.0$, $p < 0.05$; Figure 2). Furthermore, the synthesis of the membrane-embedded undecaprenyl phosphate [Und-P], also known as bactoprenol, was remarkably disturbed ($log_2FC = 2.11$) 6 h after ceftazidime/avibactam treatment, indicative that ceftazidime/avibactam antibacterial killing might involve an impairment of the essential membrane steps of peptidoglycan biosynthesis, including lipid I formation. Lipid I is formed by the transfer of the phospho-MurNAc-pentapeptide from the UDP-MurNAc-pentapeptide [UDP-MurNAc-L-Ala-γ-D-Glu-m-Dap-D-Ala-D-Ala] to lipid carrier undecaprenyl phosphate.[40,41] This process is mediated by a membrane enzyme MraY (phospho-MurNAc-pentapeptide translocase, encoded by the structural gene *mraY*) for which five classes of natural antibiotics with various modes of inhibition have been developed (e.g., muraymycin and tunicamycin).[41] Notably, ceftazidime/avibactam displayed

https://doi.org/10.1021/acsinfecdis.3c00264
ACS Infect. Dis. 2023, 9, 2409−2422

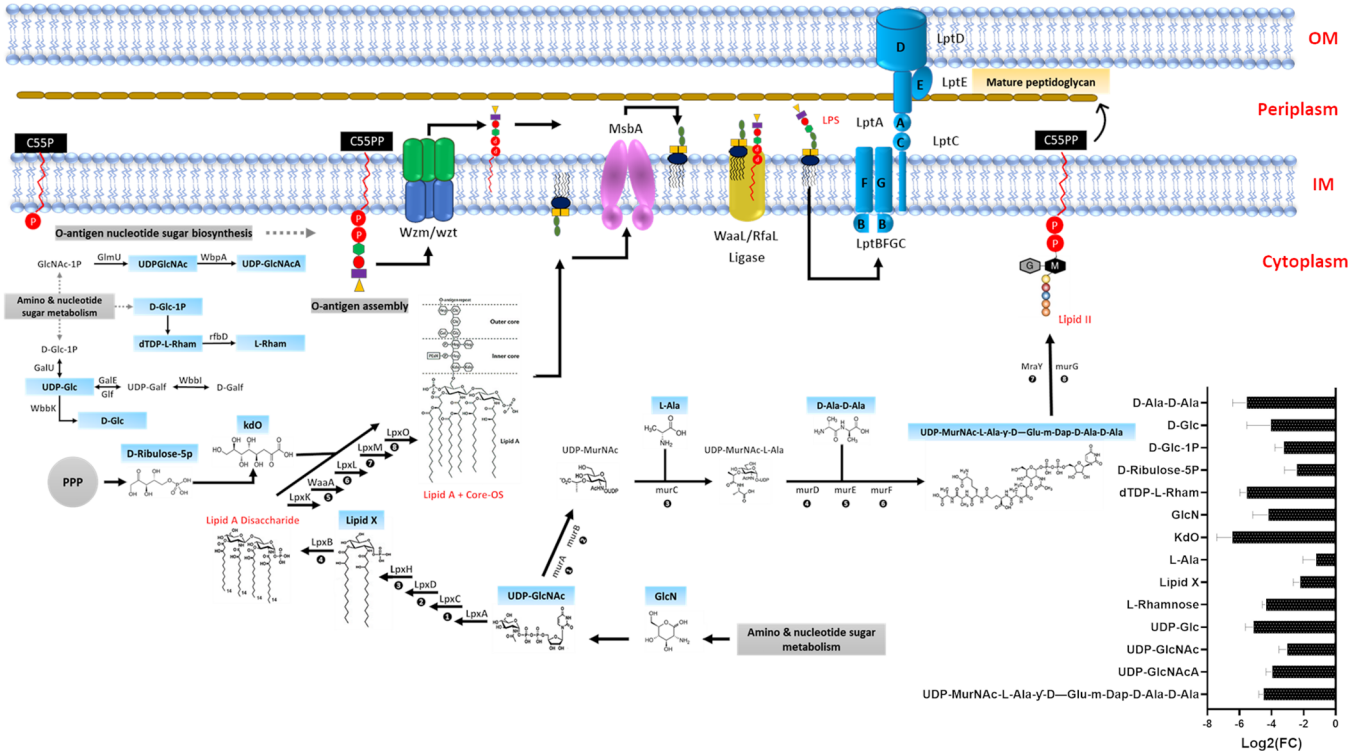

Figure 3. Comparative metabolome mapping of PDR *K. pneumoniae* FADD-KP070 responses to treatment with ceftazidime/avibactam (48/4 mg/L) at 6 h ($log_2FC \geq 0.59$ or ≤ -0.59, $p < 0.05$). Schematic and bar chart representations of all significantly affected metabolites involved in lipopolysaccharide (LPS) and *O*-antigen assembly. Blue rectangles represent the downregulated metabolites. UDP-GlcNAcA = UDP-*N*-acetyl-2-amino-2-deoxy-D-glucuronate.

no effect on intermediates [except for UDP-GlcNAc, $log_2FC= -3.10$ (3 h)] involved in the peptidoglycan biosynthetic pathway at early time exposure 1 and 3 h.

Transcriptomics data revealed that ceftazidime/avibactam treatment significantly altered six genes of Mur ligases (*murA* and *murCDEFG*) and phospho-MurNAc-pentapeptide translocase gene (*mraY*) ($log_2FC> 1.0$, FDR < 0.05; Figure 2). These genes play crucial roles in catalyzing essential reactions in peptidoglycan biosynthesis.[42,43] For example, in other studies, the downregulation of MurG, which encodes an essential glycosyltransferase catalyzing final intracellular step of peptidoglycan synthesis,[44] prevents the transfer of GlcNAc to the lipid I intermediate. This ultimately leads to a complete shutdown of peptidoglycan synthesis.[44]

Although the strain was resistant to meropenem (Table S1), we did not detect carbapenemase genes. Unsurprisingly, the expression of two extended-spectrum class A β-lactamase genes, namely, bla_{SHV-2} and bla_{SHV-4} (targeted by avibactam), showed significant downregulation in response to treatment with ceftazidime/avibactam (Figure 1B), which, in the absence of avibactam, pose a high level of resistance toward ceftazidime.[45] Notably, ceftazidime/avibactam treatment caused a marked upregulation in the level of the β-lactamase-like protein *ytnp* at 3 and 6 h ($Log_2FC= 1.24$ and 1.98, respectively; Figure 1B). No alteration in the expression of genes related to peptidoglycan formation and β-lactam resistance was detected in response to treatment at 1 h.

Lipopolysaccharide (LPS) and O-Antigen Biosynthesis. LPS is the main constituent of the Gram-negative bacteria outer membrane, contributing to the structural integrity of bacteria and protecting the membrane from environmental insults. LPS is composed of lipid A, core oligosaccharides (outer and inner), and *O*-antigen.[46]

Intriguingly, the levels of two essential amino sugars (UDP-GlcNAc and GlcN) required for the initial steps of LPS biogenesis significantly decreased 6 h after ceftazidime/avibactam treatment ($log_2FC > -3.0$, FDR < 0.05; Figure 3).

This is likely to have disturbed downstream pathways such as lipid A disaccharide formation and indeed ceftazidime/avibactam significantly decreased the abundance of *N*-acyl-D-glucosamine 1-phosphate (lipid X), a key precursor in lipid A biosynthesis,[47] D-ribulose 5-phosphate (D-ribulose-5P), a central metabolite for generating the LPS backbone, and the inner core of the LPS, namely, 3-deoxy-D-manno-octulosonate (KDO) at 6h ($log_2FC > -2.0$, FDR < 0.05; Figure 3).[48] In line with these findings, it has previously been shown that ceftazidime could disorganize and release a significant amount of LPS from the outer membranes of Gram-negative bacteria.[49−51] In vitro exposure of *P. aeruginosa* to ceftazidime resulted in a 40-fold greater increase in LPS release compared with antibiotic free controls.[51,52] Furthermore, in their in vitro study with *E. coli*, Dofferhoff et al. found that other β-lactams (e.g., cefuroxime and aztreonam) can also induce extensive endotoxin release.[53]

Our metabolomics data analysis also demonstrated that ceftazidime/avibactam perturbed another essential pathway responsible for *O*-antigen assembly during LPS formation, namely, *O*-antigen nucleotide sugar biosynthesis. The abundance of six fundamental building blocks of *O*-antigen nucleotide sugar biosynthesis [e.g., UDP-*N*-acetyl-2-amino-2-deoxy-D-glucuronate (UDP-GlcNAcA), dTDP-L-rhamnose (dTDP-L-Rham) and D-glucose 1-phosphate (D-Glc-1P)]

https://doi.org/10.1021/acsinfecdis.3c00264
ACS Infect. Dis. 2023, 9, 2409−2422

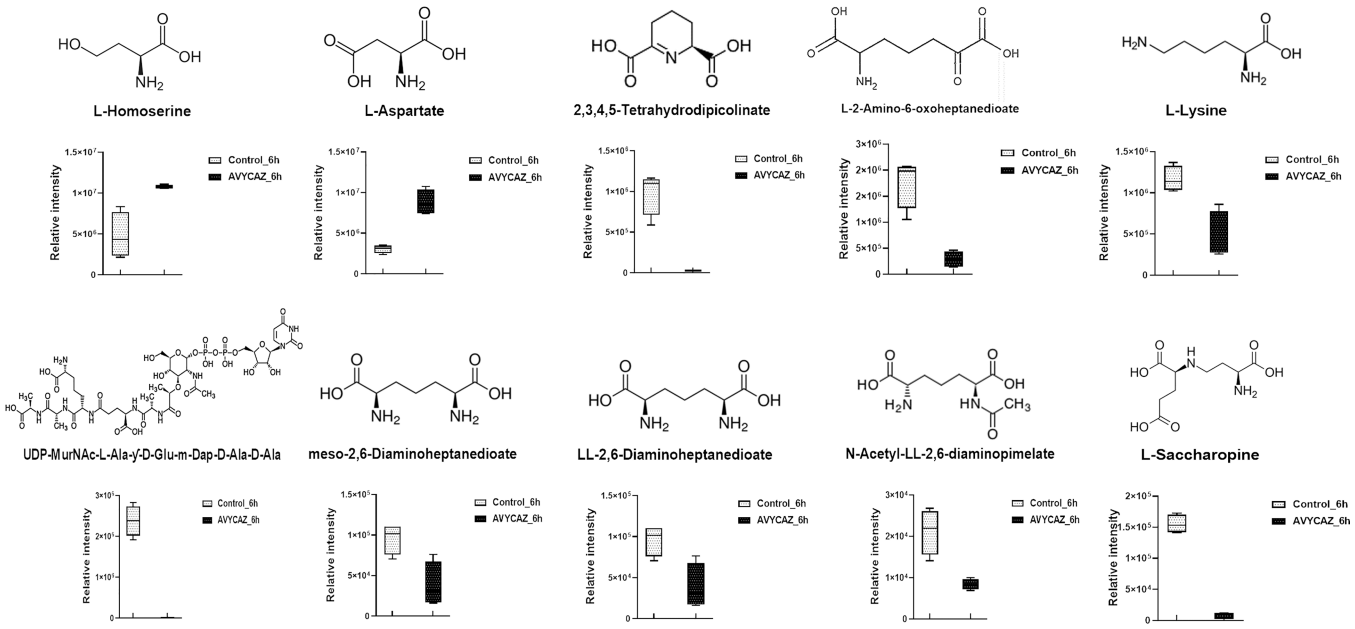

Figure 4. Box and whiskers graphs representing significantly impacted intermediates involved in lysine biosynthesis of *K. pneumoniae* FADDI-KP070 after ceftazidime/avibactam (48/4 mg/L) treatment at 6 h ($log_2FC \geq 0.59$ or ≤ -0.59, $p < 0.05$).

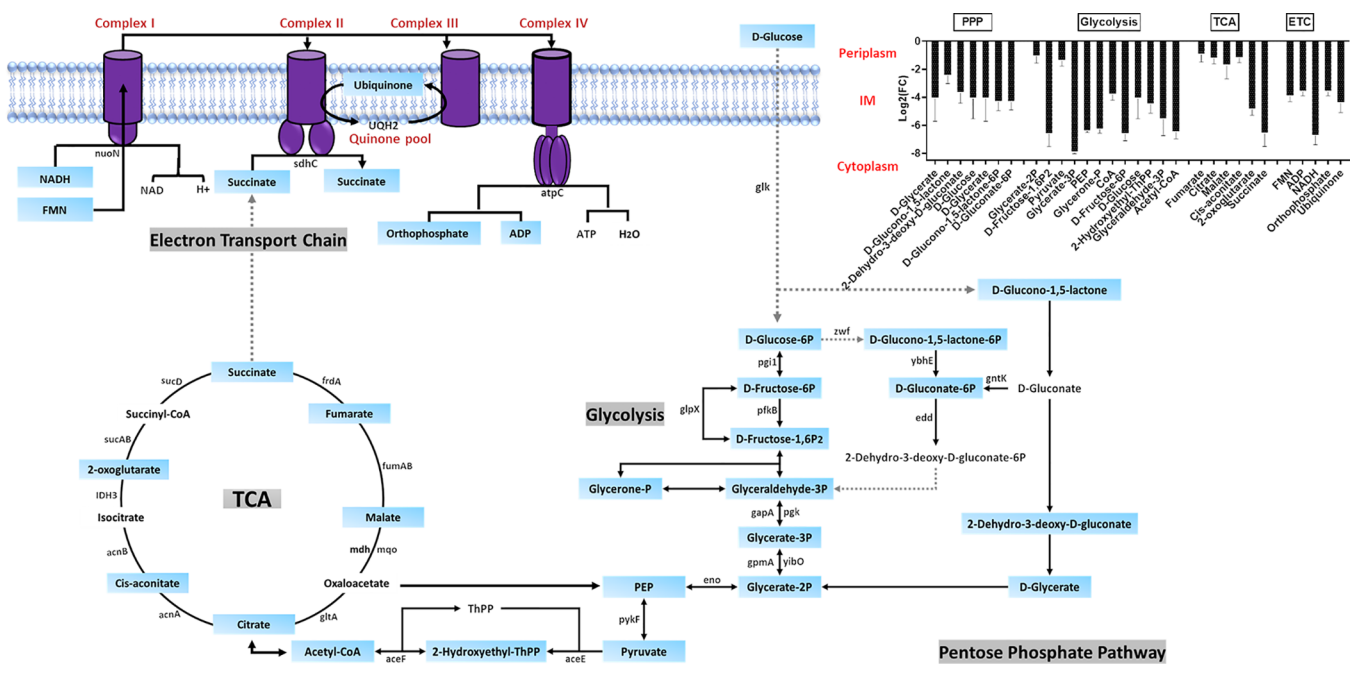

Figure 5. Schematic pathway diagram depicting significantly influenced precursors of the complex interplay metabolic pathways of central carbon metabolism [glycolysis, pentose phosphate pathway (PPP), tricarboxylic acid (TCA) cycle, and electron transport chain (ETC)] of *K. pneumoniae* FADDI-KP070 after ceftazidime/avibactam treatment at 6 h ($log_2FC \geq 0.59$ or ≤ -0.59, $p < 0.05$). Blue rectangles represent the suppressed metabolites.

were only suppressed 6 h post ceftazidime/avibactam treatment ($log_2FC \geq -3.0$, FDR < 0.05; Figure 3).

In line with the metabolomics results, we detected significant DEGs related to LPS and *O*-antigen nucleotide sugar biosynthesis in response to ceftazidime/avibactam treatment particularly at 6 h, whereas the effect was minimal at 1 and 3 h (Figure 1C). Notably, at 6 h, ceftazidime/avibactam significantly upregulated the essential genes *lpxA* and *lpxD* encoding proteins involved in the formation of lipid A, which anchors LPS to the outer membrane ($log_2FC \geq 1.0$, FDR < 0.05; Figure 1C).[54] Importantly, three genes (*lpxL*, *lpxK*, and *lpxO*), encoding enzymes responsible for the catalysis of the last sequential steps required to assemble the Kdo2−hexa-acylated lipid A of *K. pneumoniae*, were up-regulated in response to ceftazidime/avibactam treatment (Figure 1C).[55] It has previously been reported that deletion of these genes is associated with a less virulent *K. pneumoniae* phenotype, with a greater antibiotic susceptibility, particularly to polymyxins.[55] The levels of the two main genes *lptE* and *lptG* of the ABC transporter LptABCDEFG complex (important proteins

https://doi.org/10.1021/acsinfecdis.3c00264
ACS Infect. Dis. 2023, 9, 2409−2422

required for translocation and sorting of LPS to the outer membrane[56]) were considerably overexpressed in response to ceftazidime/avibactam treatment (Figure 1C). By comparison, at 1 and 3 h, the treatment induced overexpression of only *lpxL* (Figure 1C). Furthermore, transcriptome analysis also demonstrated that ceftazidime/avibactam dysregulated several genes involved in nucleotide sugar precursor synthesis and *O*-antigen assembly, namely, *galE*, *galU*, *glmU*, *glf*, and *rfbD* at 3 and 6 h (Figure 1C).

Metabolic and Transcriptomic Perturbations of Lysine Biosynthesis. Lysine biosynthesis is the central hub for supplying the main precursors lysine and *meso*-diaminopimelate (*m*-DAP) used in the biogenesis of the peptidoglycan layer of Gram-positive and Gram-negative bacteria, respectively.[57] Therefore, this pathway represents an attractive target for the development of novel antibacterial drugs.[20,57,58] Ceftazidime/avibactam treatment significantly reduced the levels of intermediate metabolites in lysine biosynthesis, including L-lysine, *meso*-2,6-diaminoheptanedioate, *N*-acetyl-LL-2,6-diaminopimelate, and LL-2,6-diaminoheptanedioate (DAP; Figure 4).

Notably, DAP levels were particularly reduced ($\log_2$FC = −1.31). Similar effects were evident in comparative transcriptome mapping which revealed that 6 h post treatment, nine essential genes of the lysine biosynthetic pathway including *dapE*, *dapB*, *dapD*, and *dapF* ($\log_2$FC ≥ 1.0, FDR < 0.05; Figure 1D) were significantly perturbed. DapE (*dapE* encoded) catalyzes the hydrolysis of *N*-succinyl-L,L-diaminopimelic acid (SDAP) to form succinate and DAP, an intermediate involved in the bacterial biosynthesis of lysine and *meso*-diaminopimelic acid, an essential component of bacterial cell walls. It has been reported that *dapE* deletion attenuates Gram-negative bacterial growth.[59,60] Therefore, there has been growing interest in DapE genes as new antimicrobial targets, notably the recently developed indoline sulfonamide DapE inhibitors.[57,61] There were no appreciable changes in the expression of genes involved in lysine biosynthesis at 1 and 3 h.

Metabolic and Transcriptomic Perturbations of Central Carbon Metabolism. Pathway analysis revealed that ceftazidime/avibactam perturbed multiple key metabolites involved in the tightly interconnected pathways of central carbon metabolism at 6 h (i.e., glycolysis, pentose phosphate pathway [PPP], tricarboxylic acid cycle [TCA], and electron transport chain [ETC]; Figure 5).

There was a significant decrease in levels of 12 fundamental building blocks of the glycolysis pathway, including D-glucose, pyruvate, phosphoenolpyruvate (PEP), acetyl-CoA, and coenzyme A (CoA) ($\log_2$FC ≥ −1.0, p < 0.05; Figure 5). Coincidently, depletion of PEP, the second source of ATP in glycolysis, and acetyl-CoA in MDR Gram-negative bacteria has been reported to potentiate the antibacterial killing effect of aminoglycosides.[62] Further, levels of crucial intermediates of the downstream PPP (e.g., D-glycerate and D-glucono-1,5-lactone) and TCA cycle (e.g., fumarate, citrate, and succinate) were significantly perturbed in response to ceftazidime/avibactam treatment (Figure 5). Concomitantly, the abundance of five key mediators of the ETC significantly decreased following ceftazidime/avibactam treatment, namely, FMN, ADP, NADH, orthophosphate, and ubiquinone ($\log_2$FC ≥ −3.0, p < 0.05; Figure 5). It has been reported that there is direct cross-talk between the TCA cycle and bacterial cell wall morphogenesis, such that any inadequacies in the availability of TCA cycle biosynthetic precursors burden peptidoglycan synthesis and ultimately increase susceptibility to β-lactams that specifically target peptidoglycan assembly.[63,64] Intriguingly, Liu et al. reported that the metabolome of ceftazidime-resistant *Vibrio alginolyticus* showed insufficiencies across the TCA cycle and disorganized cellular respiration compared with its paired susceptible strain, suggesting a potential role for these metabolic pathways in the development of ceftazidime resistance.[31] No significant changes were seen in central carbon metabolism following ceftazidime/avibactam treatment for 1 and 3 h.

The transcriptomic responses were consistent with metabolomics analysis, wherein ceftazidime/avibactam treatment induced marked dysregulation in the levels of genes related to central carbon metabolism (i.e., glycolysis, PPP, TCA cycle, and ETC) at 6 h (Figure 1E−G). Notably, the expression of genes involved in glycolysis (5 genes) and PPP (2 genes) were significantly overexpressed 6 h following treatment ($\log_2$FC ≥ 0.6, FDR < 0.05; Figure 1E). At 3 h, only two genes (*glpX* and *eno*) were perturbed in response to ceftazidime/avibactam therapy. Notably, ceftazidime/avibactam dramatically dysregulated the expression of 12 genes (e.g., *aceE*, *aceF* and *sucABD*) in the TCA cycle, as well as three essential genes (e.g., *atpC*) in the ETC ($\log_2$FC ≥ 1.0, FDR < 0.05; Figure 1F,G). ΔaceE *Escherichia coli* has been reported to display a reduced susceptibility to cationic antimicrobial peptides compared with parent wild type *E. coli*, suggesting a role for *aceE* in conferring metabolic resistance toward antimicrobial agents.[65] Furthermore, mutations in *atpC* of the ETC can mediate antimicrobial resistance in Gram-negative and Gram-positive bacteria.[66,67] Ceftazidime/avibactam treatment had no impact on the expression of genes involved in the central carbon metabolism pathways at 1 h.

Peptidoglycan Detection Assay. To determine if ceftazidime/avibactam disruption of the peptidoglycan biosynthetic pathway resulted in altered levels of cell-associated peptidoglycan, total peptidoglycan abundance was compared between untreated and ceftazidime/avibactam treated *K. pneumoniae*. Although the results showed no significant difference between the untreated and ceftazidime/avibactam treated cultures at 1 h, peptidoglycan abundance was significantly decreased at 3 h and further depleted at 6 h post-treatment (Figure 6).

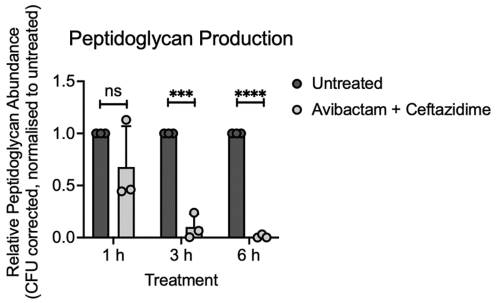

Figure 6. Detection of peptidoglycan from cultures of *K. pneumoniae* FADDI-KP070 grown either untreated or supplemented with ceftazidime/avibactam (6x MIC, 48/4 mg/L) at 1, 3, and 6 h postinoculation. Data represent the mean ± standard deviation of three independent biological experiments. Statistical significance was determined by a two-tailed unpaired *t* test, ns = not significant, *** = p < 0.0005, **** = p < 0.0001.

https://doi.org/10.1021/acsinfecdis.3c00264
ACS Infect. Dis. 2023, 9, 2409−2422

These data are consistent with the known mechanism of ceftazidime action on bacterial peptidoglycan synthesis.[68] Further, these findings confirm the observed metabolic and transcriptomic disruptions elicited by ceftazidime/avibactam and highlight the profound impact on *K. pneumoniae* peptidoglycan production. The dynamic trend observed in peptidoglycan abundance closely paralleled the patterns observed in the metabolomics and transcriptomics results, indicating a time-dependent perturbation profile. Notably, the perturbations were relatively modest at the early time point (1 h) and became significantly more heightened at the later time point (6 h). Collectively, these findings provide direct support for the mechanism of ceftazidime/avibactam action and how it influences bacterial peptidoglycan synthesis.

CONCLUSIONS

The present study investigated the integrated metabolomic-transcriptomic response of a uropathogenic clinical *K. pneumouniae* PDR isolate in response to ceftazidime/avibactam. Our novel findings identified that ceftazidime/avibactam treatment perturbed cell envelope biogenesis, bacterial membrane lipid metabolism, and central carbon metabolism. The impact of treatment on peptidoglycan biosynthetic precursors was further validated using a direct peptidoglycan detection assay. These observed perturbations seem to contribute as integral components to the potential bactericidal activity of ceftazidime/avibactam. These findings provide insight into mechanisms of action/resistance of ceftazidime/avibactam in PDR *K. pneumoniae* and also support future development of novel β-lactam/β-lactamase inhibitor combinations that can prevent or manage infections caused by this problematic pathogen.

METHODS

Bacterial Strains. PDR *K. pneumoniae* FADDI-KP070 (ceftazidime > 128 mg/L) was obtained from the SUNY Downstate Medical Center (Brooklyn, NY) from a patient with UTI. The antibiotic susceptibility antibiogram for this isolate is shown in Table S1. The isolate was stored in tryptone soy broth (Oxoid, Thermo Fisher Scientific, Waltham, MA) with 20% glycerol (Ajax Finechem, Seven Hills, NSW, Australia) in cryovials at −80 °C. The strain was subcultured onto nutrient-rich agar plates (Media Preparation Unit, University of Melbourne, Melbourne, VIC, Australia) and incubated at 37 °C for 24 h prior to use.

Antibiotics and Reagents. Cation-adjusted Mueller-Hinton broth (CAMHB, Oxoid) supplemented with calcium and magnesium (25.0 mg/L Ca^{2+}, 12.5 mg/L Mg^{2+}) was used for susceptibility testing and in vitro experiments. Stock solutions of ceftazidime (Selleckchem, Houston, TX; Catalog No. S3649) and avibactam sodium (Selleckchem, Houston, TX; Catalog No. S3732) were prepared using Milli-Q water (Millipore, Australia). All drug solutions were filter-sterilized using a 0.22-μm filter (Sartorius, Australia). All other reagents were purchased from Sigma-Aldrich (Australia) and were of the highest commercial grade available.

Determination of Minimum Inhibitory Concentrations (MICs). MICs were determined in triplicate using the broth microdilution method, in accordance with the Clinical and Laboratory Standards Institute (CLSI).[69] In all experiments, ceftazidime−avibactam MIC values were established by employing double dilutions of ceftazidime while upholding a steady concentration of 4 μg/mL of avibactam.[6,70]

Bacterial Culture Preparation for Metabolomics and Transcriptomics. Late exponential (~10^8 CFU/mL) time-kill assays were carried out in triplicate to characterize the pharmacodynamic activity of ceftazidime/avibactam and optimize the experimental conditions (Figure S1).[36] To ensure the appropriateness of bacterial counts for omics studies, a higher starting inoculum of *K. pneumoniae* FADDI-KP070 (~10^8 CFU/mL) was employed to avoid excessive bacterial killing. During the optimization phase, the logarithmic phase bacterial culture was exposed to varying concentrations of ceftazidime/avibactam [1 × MIC (mg/L): 8/4; 2 × MIC (mg/L): 16/4; 4 × MIC (mg/L): 32/4; 6 × MIC (mg/L): 48/4; 8 × MIC (mg/L): 64/4. Notably, the concentration of 6xMIC of ceftazidime/avibactam (48 mg/4/L) emerged as the optimal choice for subsequent omics studies (Figure S1). For the preparation of omics bacterial samples, exponential phase broth cultures were prepared prior to each experiment by adding fresh *K. pneumoniae* FADDI-KP070 colonies from overnight growth to prewarmed CAMHB (37 °C) to achieve the desired initial inoculum of ~10^8 CFU/mL (OD_{600} ~ 0.5). Ceftazidime/avibactam was added to the logarithmic phase bacterial culture to achieve the appropriate ceftazidime/avibactam (6x MIC, 48/4 mg/L) concentrations. Each 200 mL culture was incubated at 37 °C in a Bioline rotary shaker (shaking speed 180 rpm), and 15 mL samples were withdrawn from each treatment group at 1, 3, and 6 h. The samples (n = 4 biological replicates, 15 mL each) were quenched rapidly on dry ice-ethanol for 30 s and subsequently normalized using fresh broth to reach the pretreatment level ~0.5. Afterward, the samples were centrifuged at 3220 x g at 4 °C for 15 min. Following centrifugation, the supernatants were discarded, and the resulting pellets were stored at a −80 freezer for subsequent metabolite extraction.

Metabolomics. *Metabolite Extraction.* Bacterial pellets were washed twice in 1 mL of 0.9% NaCl followed by centrifugation at 3220 × g at 4 °C for 5 min to remove residual extracellular metabolites. Chloroform−methanol−water (250 μL) (1:3:1 v/v/v) extraction solvent containing 1 μM each of the internal standards (CHAPS, CAPS, PIPES, and TRIS) was added to the resuspended pellets. These internal standards were selected as they are physiochemically diverse small molecules that do not naturally occur in any known microorganism. Samples were then frozen three times in liquid nitrogen, thawed on ice, and then vortexed to release the intracellular metabolites. After the third cycle, samples were centrifuged again for 10 min at 3220 × g at 4 °C, wherein the supernatants were transferred into 1.5 mL Eppendorf tubes for immediate storage at −80 °C. Prior to analysis, samples were thawed and centrifuged at 14,000 × g at 4 °C for 10 min to remove any particulate matter, and then, 200 μL of the sample was transferred into the injection vial for LC−MS analysis. An equal volume of each sample was combined for use as a quality control sample so that a sample contained all analytes during the analysis.[71] It is important to recognize that certain alterations might occur in the metabolites during the experimental processes involving quenching, centrifugation, and extraction.

LC−MS Analysis. Hydrophilic interaction liquid chromatography (HILIC) high-resolution mass spectrometry using a Dionex high-performance liquid chromatography system (RSLCU3000, Thermo Fisher Scientific) with a ZIC-PHILIC

https://doi.org/10.1021/acsinfecdis.3c00264
ACS Infect. Dis. 2023, 9, 2409−2422

column (5 μm, polymeric, 150 × 4.6 mm; SeQuant, Merck, Darmstadt, Germany) was employed for identifying polar metabolites. The system was linked to a Q-Exactive Orbitrap mass spectrometer (Thermo Fisher Scientific) equipped with positive and negative electrospray (ESI) modes at 35000 resolutions with a mass range of 85 to 1275 m/z. The LC solvents were (A) 20 mM ammonium carbonate and (B) acetonitrile, operated via a multistep gradient system. The gradient system started at 80% B and was decreased to 50% B over 15 min, then reduced from 50% B to 5% B over 3 min, thereafter washed with 5% B for another 3 min, and finally 8 min re-equilibration with 80% B at a flow rate of 0.3 mL/min.[72] The cycle time was 32 min with an injection sample volume of 10 μL. To avoid batch-to-batch variation, all samples were analyzed as a single LC−MS batch. A mixture containing over 250 metabolites used as pure standards was processed as a part of the analysis batch to help with metabolite identification.

Data Processing, Bioinformatics, and Statistical Analyses. Raw mass spectrometry data were processed using IDEOM (http://mzmatch.sourceforge.net/ideom.php)[73] employing ProteoWizard to convert the raw LC-MS data into a.mzXML format. XCMS is a freely available software package used for raw peak detection, while Mzmatch.R, is a software package developed to extend the capabilities of XCMS[74,75] to align samples and filter peaks using a minimum peak intensity threshold of 100,000 with a relative standard deviation (RSD) of <0.5 (reproducibility). Mzmatch.R was also used to retrieve any missing peaks and to annotate related peaks. Noise and artifact peaks were removed using default IDEOM parameters. While loss of a proton was corrected in negative ESI mode, the gain of a proton was corrected in positive ESI mode, followed by identification of metabolites based on their exact mass within 2 ppm. The identification of each metabolite (Level 1 identification based on MSI standards) was confirmed using the retention rates of authentic standards. Other metabolites were identified (Level 2 identification based on MSI standards) using exact mass and predicted retention time based on the Kyoto Encyclopedia of Genes and Genomes (KEGG; http://www.genome.jp/kegg/), MetaCyc, and LIPIDMAPS databases. In cases where isomers could not be clearly differentiated by retention time, bacterial metabolites annotated in EcoCyc were preferentially selected. MetaboAnalyst 5.0, a free online tool used for performing statistical analysis (https://www.metaboanalyst.ca). Putative metabolites with a median RSD ≤ 0.2 (20%) within the QC group and IDEOM confidence level ≥5 were incorporated into a table and then uploaded to MetaboAnalyst. Half of the minimum positive values in the original data were used to replace features with >25% missing values. The interquartile range was used to filter the data followed by $\log_2$ transformation and auto scaling to normalize the data. One-way ANOVA ($p < 0.05$ for Fisher's LSD; fold change threshold = 1.5) was used to identify metabolites with significant changes between control and treatment groups. KEGG mapper was used to build the metabolic pathway modules by uploading the KEGG IDs of the statistically significant metabolites.

RNA Extraction and Analysis of RNA Sequencing Data. For RNA analysis, a further 1.5 mL sample was taken from each treatment group at 1, 3, and 6 h for RNA extraction. RNA was extracted according to the RNeasy Mini Kit protocol (Qiagen, Hilden, Germany). Libraries were prepared with the Nextera library preparation kit, using a previously described protocol.[76] Samples were sequenced using an Illumina HiSeq 1500 at Genewiz (paired-end 150 bp, Illumina HiSeq, Suzhou, China). The raw reads were aligned to the strain genome using Rsubread v2.6.3. Counts of mapped reads were summarized by featureCounts. Differential gene expression was identified using voom and limma linear modeling methods via a web-based RNA-seq visualization software Degust (http://degust.erc.monash.edu).[77] Statistical significance of differential gene expression (DEG) was defined using a cutoff of $\log_2$FC ≥ 0.59 or ≤ −0.59 and false discovery rate (FDR) < 0.05. PCA plots and Venn diagrams were generated using customized R scripts and GeneVenn, respectively.[78] Gene ontology and pathway analysis of DEGs were performed using the KEGG (http://www.genome.jp/kegg/) and BioCyc (https://biocyc.org/). It is noteworthy to mention that β-lactamase genes (bla_{SHV-2} and bla_{SHV-4}) were detected in the tested strain by using standard β-lactamase nomenclature.

Peptidoglycan Detection Assay. Detection of peptidoglycan was conducted using a muramic acid quantitation protocol modified from a previous study.[79] Briefly, *K. pneumoniae* FADDI-KP070 was cultured on tryptic soy agar (TSA) at 37 °C with overnight biomass inoculated into 10 mL of prewarmed CAMHB at a starting optical density (OD_{600}) of 0.5. Cultures were supplemented with ceftazidime/avibactam (6 × MIC, 48/4 mg/L) or left untreated. Cultures were incubated at 37 °C in an Innova shaking incubator (shaking speed 180 rpm) and 1 mL samples were withdrawn from each treatment group at 1, 3, and 6 h post inoculation. The OD_{600} for each sample was measured and normalized to ∼0.5 with fresh CAMHB. The cultures were harvested via centrifugation at 18,000 × g for 4 min and washed once in 1 mL of sterile PBS with 20 μL taken for CFU enumeration. The cell pellets were resuspended in 100 μL of 1 M NaOH and left to incubate at 38 °C for 30 min, prior to the addition of 100 μL of 0.5 M H_2SO4 and 1 mL of concentrated H_2SO4 (∼18 M). Samples were incubated at 96 °C for 7 min and cooled on ice prior to the addition of 10 μL of 4% [w/v] $CuSO_4$ and 20 μL of 1.5% [w/v] 4-phenylphenol in 96% ethanol with immediate mixing. Samples were then incubated for a further 30 min at 30 °C before the determination of OD_{560} in a clear, 96-well plate using a CLARIOStar spectrophotometer (BMG Labtech). CFU was enumerated after overnight growth on TSA plates at 37 °C, and OD_{560} was corrected for CFU/mL for each culture and normalized to untreated. Statistical analyses were performed in GraphPad Prism version 10.0.1.

■ ASSOCIATED CONTENT

Data Availability Statement

The data supporting the findings of this study are available in the supplementary materials, and the raw data and analysis scripts are deposited in a publicly accessible repository, GenBank and the Sequence Read Archive (SRA), accession number PRJNA1035254.

Supporting Information

The Supporting Information is available free of charge at https://pubs.acs.org/doi/10.1021/acsinfecdis.3c00264.

Time-kill curve for different concentrations of ceftazidime/avibactam; total acquired metabolites detected through comprehensive profiling and the proportion of each metabolite class; PCA plots for metabolite levels from *K. pneumoniae* FADDI-KP070 samples treated with ceftazidime/avibactam at 1, 3, and 6 h; volcano plots depicting the total number of significant metabolites

https://doi.org/10.1021/acsinfecdis.3c00264
ACS Infect. Dis. 2023, 9, 2409−2422

after ceftazidime/avibactam treatment of *K. pneumoniae* FADDI-KP070 at 1, 3, and 6 h; summary of significantly changed metabolites of *K. pneumoniae* FADDI-KP070 from different categories following ceftazidime/avibactam treatment at 1, 3, and 6 h; Venn diagrams showing the number of metabolites significantly affected by each treatment for *K. pneumoniae* FADDI-KP070 at 1, 3, and 6 h; PCA plots for *K. pneumoniae* FADDI-KP070 transcriptome after ceftazidime/avibactam at 1, 3, and 6 h; total numbers of differentially expressed genes (DEGs) of *K. pneumoniae* FADDI-KP070 after ceftazidime/avibactam treatment at 1, 3, and 6 h; Venn diagrams showing the number of differentially expressed genes (DEGs) induced by ceftazidime/avibactam treatment of *K. pneumoniae* FADDI-KP070 at 1, 3, and 6 h; antibiogram of the clinical isolate *K. pneumoniae* FADDI-KP070; and differentially expressed genes (DEGs) of *K. pneumoniae* FADD-KP070 after ceftazidime/avibactam treatment (PDF)

AUTHOR INFORMATION

Corresponding Authors

Jian Li − *Monash Biomedicine Discovery Institute, Department of Microbiology, Monash University, Clayton, Victoria 3800, Australia;* orcid.org/0000-0001-7953-8230; Email: Jian.li@monash.edu

Tony Velkov − *Monash Biomedicine Discovery Institute, Department of Microbiology, Monash University, Clayton, Victoria 3800, Australia;* orcid.org/0000-0002-0017-7952; Email: Tony.velkov@monash.edu

Authors

Maytham Hussein − *Monash Biomedicine Discovery Institute, Department of Microbiology, Monash University, Clayton, Victoria 3800, Australia;* orcid.org/0000-0001-5922-7312

Rafah Allobawi − *Monash Biomedicine Discovery Institute, Department of Microbiology, Monash University, Clayton, Victoria 3800, Australia*

Jinxin Zhao − *Monash Biomedicine Discovery Institute, Department of Microbiology, Monash University, Clayton, Victoria 3800, Australia*

Heidi Yu − *Monash Biomedicine Discovery Institute, Department of Microbiology, Monash University, Clayton, Victoria 3800, Australia*

Stephanie L. Neville − *Department of Microbiology and Immunology, The Peter Doherty Institute for Infection and Immunity, The University of Melbourne, Melbourne, Victoria 3010, Australia*

Jonathan Wilksch − *Department of Microbiology and Immunology, The Peter Doherty Institute for Infection and Immunity, The University of Melbourne, Melbourne, Victoria 3010, Australia*

Labell J. M. Wong − *Monash Biomedicine Discovery Institute, Department of Microbiology, Monash University, Clayton, Victoria 3800, Australia*

Mark Baker − *Discipline of Biological Sciences, Priority Research Centre in Reproductive Biology, Faculty of Science and IT, University of Newcastle, Callaghan, NSW 2308, Australia*

Christopher A. McDevitt − *Department of Microbiology and Immunology, The Peter Doherty Institute for Infection and Immunity, The University of Melbourne, Melbourne, Victoria 3010, Australia;* orcid.org/0000-0003-1596-4841

Gauri G. Rao − *Division of Pharmacotherapy and Experimental Therapeutics, Eshelman School of Pharmacy, University of North Carolina, Chapel Hill, North Carolina 27599-7355, United States;* orcid.org/0000-0002-8704-7770

Complete contact information is available at: https://pubs.acs.org/10.1021/acsinfecdis.3c00264

Funding

G.G.R., T.V., and J.L. were supported by the National Institute of Allergy and Infectious Diseases, award numbers R01AI146241 and R01AI170889. The content is solely the responsibility of the authors and does not necessarily represent the official views of the National Institutes of Health.

Notes

The authors declare no competing financial interest.

ACKNOWLEDGMENTS

J.L. is an Australian National Health and Medical Research Council (NHMRC) Principal Research Fellow, and T.V. is an Australian REDI MPT Connect Fellow. J.Z. is a recipient of the 2022 Faculty of Medicine, Nursing and Health Sciences Bridging Fellowship, Monash University.

REFERENCES

(1) EclinicalMedicine. EclinicalMedicine, Antimicrobial resistance: a top ten global public health threat. *eClinicalMedicine* **2021**, *41*, 101221,

(2) Magill, S. S.; Edwards, J. R.; Bamberg, W.; Beldavs, Z. G.; Dumyati, G.; Kainer, M. A.; Lynfield, R.; Maloney, M.; McAllister-Hollod, L.; Nadle, J.; Ray, S. M.; Thompson, D. L.; Wilson, L. E.; Fridkin, S. K. Multistate point-prevalence survey of health care-associated infections. *New Engl. J. Med.* **2014**, *370* (13), 1198−208.

(3) Sidjabat, H.; Nimmo, G. R.; Walsh, T. R.; Binotto, E.; Htin, A.; Hayashi, Y.; Li, J.; Nation, R. L.; George, N.; Paterson, D. L. Carbapenem resistance in *Klebsiella pneumoniae* due to the New Delhi Metallo-β-lactamase. *Clin. Infect. Dis.* **2011**, *52* (4), 481−484.

(4) Arnold, R. S.; Thom, K. A.; Sharma, S.; Phillips, M.; Kristie Johnson, J.; Morgan, D. J. Emergence of *Klebsiella pneumoniae* carbapenemase-producing bacteria. *South Med. J.* **2011**, *104* (1), 40−45.

(5) Borer, A.; Saidel-Odes, L.; Riesenberg, K.; Eskira, S.; Peled, N.; Nativ, R.; Schlaeffer, F.; Sherf, M. Attributable mortality rate for carbapenem-resistant *Klebsiella pneumoniae* bacteremia. *Infect. Control Hosp. Epidemiol.* **2009**, *30* (10), 972−976.

(6) Mosley, J. F., 2nd; Smith, L. L.; Parke, C. K.; Brown, J. A.; Wilson, A. L.; Gibbs, L. V. Ceftazidime-Avibactam (Avycaz): For the Treatment of Complicated Intra-Abdominal and Urinary Tract Infections. *P T* **2016**, *41* (8), 479−483.

(7) Richards, D. M.; Brogden, R. N. Ceftazidime. A review of its antibacterial activity, pharmacokinetic properties and therapeutic use. *Drugs* **1985**, *29* (2), 105−161.

(8) Nichols, W. W.; Bradford, P. A.; Stone, G. G. The primary pharmacology of ceftazidime/avibactam: *in vivo* translational biology and pharmacokinetics/pharmacodynamics (PK/PD). *J. Antimicrob. Chemother.* **2022**, *77* (9), 2341−2352.

(9) Das, S.; Li, J.; Riccobene, T.; Carrothers, T. J.; Newell, P.; Melnick, D.; Critchley, I. A.; Stone, G. G.; Nichols, W. W., Dose selection and validation for ceftazidime-avibactam in adults with complicated intra-abdominal infections, complicated urinary tract infections, and nosocomial pneumonia. *Antimicrob. Agents Chemother.* **2019**, *63* (4), e02187-18, DOI: 10.1128/AAC.02187-18

(10) Richards, D. M.; Brogden, R. Ceftazidime. *Drugs* **1985**, *29* (2), 105−161.

(11) Bradford, P. A.; Huband, M. D.; Stone, G. G., A Systematic Approach to the Selection of the Appropriate Avibactam Concentration for Use with Ceftazidime in Broth Microdilution Susceptibility Testing. *Antimicrob. Agents Chemother.* **2018**, *62* (7), 00223-18, DOI: 10.1128/AAC.00223-18
(12) Organization, W. H. *World Health Organization model list of essential medicines for children: 7th list 2019*; World Health Organization: 2019.
(13) Fontana, C.; Favaro, M.; Campogiani, L.; Malagnino, V.; Minelli, S.; Bossa, M. C.; Altieri, A.; Andreoni, M.; Sarmati, L., Ceftazidime/Avibactam-Resistant *Klebsiella pneumoniae* subsp. pneumoniae Isolates in a Tertiary Italian Hospital: Identification of a New Mutation of the Carbapenemase Type 3 (KPC-3) Gene Conferring Ceftazidime/Avibactam Resistance. *Microorganisms* **2021**, *9* (11), 2356, DOI: 10.3390/microorganisms9112356
(14) Räisänen, K.; Koivula, I.; Ilmavirta, H.; Puranen, S.; Kallonen, T.; Lyytikäinen, O.; Jalava, J., Emergence of ceftazidime-avibactam-resistant Klebsiella pneumoniae during treatment, Finland, December 2018. *Euro Surveill* **2019**, *24* (19), 1900256, DOI: 10.2807/1560-7917.ES.2019.24.19.1900256
(15) Shi, Q.; Han, R.; Guo, Y.; Yang, Y.; Wu, S.; Ding, L.; Zhang, R.; Yin, D.; Hu, F. Multiple Novel Ceftazidime-Avibactam-Resistant Variants of bla KPC-2-Positive *Klebsiella pneumoniae* in Two Patients. *Microbiol. Spectrum* **2022**, *10* (3), No. e0171421.
(16) Gray, D. A.; Wenzel, M. Multitarget Approaches against Multiresistant Superbugs. *ACS Infect. Dis.* **2020**, *6* (6), 1346−1365.
(17) Zhao, S.; Iyengar, R. Systems pharmacology: network analysis to identify multiscale mechanisms of drug action. *Annu. Rev. Pharmacol. Toxicol.* **2012**, *52*, 505−521.
(18) Balleza, E.; Lopez-Bojorquez, L. N.; Martínez-Antonio, A.; Resendis-Antonio, O.; Lozada-Chávez, I.; Balderas-Martínez, Y. I.; Encarnación, S.; Collado-Vides, J. Regulation by transcription factors in bacteria: beyond description. *FEMS Microbiol. Rev.* **2009**, *33* (1), 133−151.
(19) Vincent, I. M.; Ehmann, D. E.; Mills, S. D.; Perros, M.; Barrett, M. P. Untargeted metabolomics to ascertain antibiotic modes of action. *Antimicrob. Agents Chemother.* **2016**, *60* (4), 2281−2291.
(20) Hussein, M.; Wong, L. J. M.; Zhao, J.; Rees, V. E.; Allobawi, R.; Sharma, R.; Rao, G. G.; Baker, M.; Li, J.; Velkov, T. Unique mechanistic insights into pathways associated with the synergistic activity of polymyxin B and caspofungin against multidrug-resistant *Klebsiella pneumoniae*. *Comput. Struct. Biotechnol. J.* **2022**, *20*, 1077−1087.
(21) Hussein, M.; Allobawi, R.; Levou, I.; Blaskovich, M. A. T.; Rao, G. G.; Li, J.; Velkov, T., Mechanisms Underlying Synergistic Killing of Polymyxin B in Combination with Cannabidiol against *Acinetobacter baumannii*: A Metabolomic Study. *Pharmaceutics* **2022**, *14* (4), 786, DOI: 10.3390/pharmaceutics14040786
(22) Hussein, M.; Han, M.-L.; Zhu, Y.; Zhou, Q.; Lin, Y.-W.; Hancock, R. E.; Hoyer, D.; Creek, D. J.; Li, J.; Velkov, T. Metabolomics study of the synergistic killing of polymyxin B in combination with amikacin against polymyxin-susceptible and-resistant *Pseudomonas aeruginosa*. *Antimicrob. Agents Chemother.* **2019**, *64* (1), No. e01587-19.
(23) Hussein, M.; Wong, L. J.; Zhao, J.; Rees, V. E.; Allobawi, R.; Sharma, R.; Rao, G. G.; Baker, M.; Li, J.; Velkov, T. Unique mechanistic insights into pathways associated with the synergistic activity of polymyxin B and caspofungin against multidrug-resistant *Klebsiella pneumoniae*. *Comput. Struct. Biotechnol. J.* **2022**, *20*, 1077−1087.
(24) Hussein, M.; Allobawi, R.; Levou, I.; Blaskovich, M. A.; Rao, G. G.; Li, J.; Velkov, T. Mechanisms underlying synergistic killing of polymyxin b in combination with cannabidiol against *Acinetobacter baumannii*: A metabolomic study. *Pharmaceutics* **2022**, *14* (4), 786.
(25) Hussein, M.; Hu, X.; Paulin, O. K. A.; Crawford, S.; Tony Zhou, Q.; Baker, M.; Schneider-Futschik, E. K.; Zhu, Y.; Li, J.; Velkov, T. Polymyxin B combinations with FDA-approved non-antibiotic phenothiazine drugs targeting multi-drug resistance of Gram-negative pathogens. *Comput. Struct. Biotechnol. J.* **2020**, *18*, 2247−2258.
(26) Zhang, Y.-M.; Rock, C. O. Membrane lipid homeostasis in bacteria. *Nat. Rev. Microbiol.* **2008**, *6* (3), 222−233.
(27) Yao, J.; Rock, C. O. Phosphatidic acid synthesis in bacteria. *Biochim. Biophys. Acta, Mol. Cell Biol. Lipids* **2013**, *1831* (3), 495−502.
(28) Casillas-Vargas, G.; Ocasio-Malavé, C.; Medina, S.; Morales-Guzmán, C.; Del Valle, R. G.; Carballeira, N. M.; Sanabria-Ríos, D. J. Antibacterial fatty acids: An update of possible mechanisms of action and implications in the development of the next-generation of antibacterial agents. *Prog. Lipid Res.* **2021**, *82*, No. 101093.
(29) Boersch, M.; Rudrawar, S.; Grant, G.; Zunk, M. Menaquinone biosynthesis inhibition: a review of advancements toward a new antibiotic mechanism. *RSC Adv.* **2018**, *8* (10), 5099−5105.
(30) Desai, J.; Liu, Y. L.; Wei, H.; Liu, W.; Ko, T. P.; Guo, R. T.; Oldfield, E. Structure, Function, and Inhibition of *Staphylococcus aureus* Heptaprenyl Diphosphate Synthase. *ChemMedChem* **2016**, *11* (17), 1915−1923.
(31) Liu, S.-R.; Peng, X.-X.; Li, H. Metabolic mechanism of ceftazidime resistance in *Vibrio alginolyticus*. *Infect. Drug Resist.* **2019**, *12*, 417.
(32) Li, X.; Liu, L.; Ji, J.; Chen, Q.; Hua, X.; Jiang, Y.; Feng, Y.; Yu, Y. Tigecycline resistance in *Acinetobacter baumannii* mediated by frameshift mutation in plsC, encoding 1-acyl-sn-glycerol-3-phosphate acyltransferase. *Eur. J. Clin. Microbiol. Infect. Dis.* **2015**, *34* (3), 625−631.
(33) Pathania, A.; Anba-Mondoloni, J.; Gominet, M.; Halpern, D.; Dairou, J.; Dupont, L.; Lamberet, G.; Trieu-Cuot, P.; Gloux, K.; Gruss, A. (p)ppGpp/GTP and Malonyl-CoA Modulate *Staphylococcus aureus* Adaptation to FASII Antibiotics and Provide a Basis for Synergistic Bi-Therapy. *mBio* **2021**, *12* (1), No. e03193-20.
(34) Nikaido, H. Molecular basis of bacterial outer membrane permeability revisited. *Microbiol. Mol. Biol. Rev.* **2003**, *67* (4), 593−656.
(35) Buijs, J.; Dofferhoff, A. S.; Mouton, J. W.; van der Meer, J. W. Continuous administration of PBP-2- and PBP-3-specific beta-lactams causes higher cytokine responses in murine *Pseudomonas aeruginosa* and *Escherichia coli* sepsis. *J. Antimicrob. Chemother.* **2007**, *59* (5), 926−933.
(36) Hussein, M.; Karas, J. A.; Schneider-Futschik, E. K.; Chen, F.; Swarbrick, J.; Paulin, O. K. A.; Hoyer, D.; Baker, M.; Zhu, Y.; Li, J.; Velkov, T., The Killing Mechanism of Teixobactin against Methicillin-Resistant *Staphylococcus aureus*: an Untargeted Metabolomics Study. *mSystems* **2020**, *5* (3), e00077-20, DOI: 10.1128/mSystems.00077-20
(37) Mikkola, S. Nucleotide Sugars in Chemistry and Biology. *Molecules* **2020**, *25* (23), 5755.
(38) Lupoli, T. J.; Tsukamoto, H.; Doud, E. H.; Wang, T. S.; Walker, S.; Kahne, D. Transpeptidase-mediated incorporation of D-amino acids into bacterial peptidoglycan. *J. Am. Chem. Soc.* **2011**, *133* (28), 10748−10751.
(39) Liu, Y.; Breukink, E., The Membrane Steps of Bacterial Cell Wall Synthesis as Antibiotic Targets. *Antibiotics* **2016**, *5* (3), 28, DOI: 10.3390/antibiotics5030028
(40) Barreteau, H.; Kovač, A.; Boniface, A.; Sova, M.; Gobec, S.; Blanot, D. Cytoplasmic steps of peptidoglycan biosynthesis. *FEMS Microbiol. Rev.* **2008**, *32* (2), 168−207.
(41) Chung, B. C.; Mashalidis, E. H.; Tanino, T.; Kim, M.; Matsuda, A.; Hong, J.; Ichikawa, S.; Lee, S.-Y. Structural insights into inhibition of lipid I production in bacterial cell wall synthesis. *Nature* **2016**, *533* (7604), 557−560.
(42) Bugg, T. D.; Lloyd, A. J.; Roper, D. I. Phospho-MurNAc-pentapeptide translocase (MraY) as a target for antibacterial agents and antibacterial proteins. *Infect. Disord.: Drug Targets* **2006**, *6* (2), 85−106.
(43) El Zoeiby, A.; Sanschagrin, F.; Levesque, R. C. Structure and function of the Mur enzymes: development of novel inhibitors. *Mol. Microbiol.* **2003**, *47* (1), 1−12.
(44) Mengin-Lecreulx, D.; Texier, L.; Rousseau, M.; van Heijenoort, J. The murG gene of Escherichia coli codes for the UDP-N-acetylglucosamine: N-acetylmuramyl-(pentapeptide) pyrophosphoryl-

undecaprenol N-acetylglucosamine transferase involved in the membrane steps of peptidoglycan synthesis. *J. Bacteriol.* **1991**, *173* (15), 4625−4636.
(45) Levasseur, P.; Girard, A. M.; Lavallade, L.; Miossec, C.; Pace, J.; Coleman, K. Efficacy of a Ceftazidime-Avibactam combination in a murine model of Septicemia caused by Enterobacteriaceae species producing ampc or extended-spectrum β-lactamases. *Antimicrob. Agents Chemother.* **2014**, *58* (11), 6490−6495.
(46) Bertani, B.; Ruiz, N., Function and Biogenesis of Lipopolysaccharides. *EcoSal Plus* **2018**, *8* (1). DOI: 10.1128/ecosalplus.ESP-0001-2018
(47) Bishop, R. E.; Gibbons, H. S.; Guina, T.; Trent, M. S.; Miller, S. I.; Raetz, C. R. Transfer of palmitate from phospholipids to lipid A in outer membranes of gram-negative bacteria. *EMBO J.* **2000**, *19* (19), 5071−5080.
(48) Regué, M.; Izquierdo, L.; Fresno, S.; Piqué, N.; Corsaro, M. M.; Naldi, T.; De Castro, C.; Waidelich, D.; Merino, S.; Tomás, J. M. A second outer-core region in *Klebsiella pneumoniae* lipopolysaccharide. *J. Bacteriol.* **2005**, *187* (12), 4198−4206.
(49) Evans, M. E.; Pollack, M. Effect of Antibiotic Class and Concentration on the Release of Lipopolysaccharide from *Escherichia coli*. *J. Infect. Dis.* **1993**, *167* (6), 1336−1343.
(50) van Langevelde, P.; Kwappenberg, K. M.; Groeneveld, P. H.; Mattie, H.; van Dissel, J. T. Antibiotic-induced lipopolysaccharide (LPS) release from *Salmonella typhi*: delay between killing by ceftazidime and imipenem and release of LPS. *Antimicrob. Agents Chemother.* **1998**, *42* (4), 739−743.
(51) Jackson, J. J.; Kropp, H. ß-Lactam Antibiotic-Induced Release of Free Endotoxin: In Vitro Comparison of Penicillin-Binding Protein (PBP) 2-Specific Imipenem and PBP 3-Specific Ceftazidime. *J. Infect. Dis.* **1992**, *165* (6), 1033−1041.
(52) Hurley, J. C.; Jackson, J. J.; KropP, H. β-Lactam Antibiotic-Induced Release of Free Lipopolysaccharide [with Reply]. *J. Infect. Dis.* **1993**, *167* (3), 775−777.
(53) Dofferhoff, A. S. M.; Nijland, J. H.; de Vries-Hospers, H. G.; Mulder, P. O. M.; Weits, J.; Bom, V. J. J. Effects of Different Types and Combinations of Antimicrobial Agents on Endotoxin Release from Gram-negative Bacteria: An *In-Vitro* and *In-Vivo* Study. *Scand. J. Infect. Dis.* **1991**, *23* (6), 745−754.
(54) Coleman, J.; Raetz, C. R. First committed step of lipid A biosynthesis in *Escherichia coli*: sequence of the lpxA gene. *J. Bacteriol.* **1988**, *170* (3), 1268−1274.
(55) Mills, G.; Dumigan, A.; Kidd, T.; Hobley, L.; Bengoechea, J. A., Identification and Characterization of Two *Klebsiella pneumoniae* lpxL Lipid A Late Acyltransferases and Their Role in Virulence. *Infect. Immun.* **2017**, *85* (9), e00068-17, DOI: 10.1128/IAI.00068-17
(56) Narita, S.; Tokuda, H. Biochemical characterization of an ABC transporter LptBFGC complex required for the outer membrane sorting of lipopolysaccharides. *FEBS Lett.* **2009**, *583* (13), 2160−2164.
(57) Gillner, D. M.; Becker, D. P.; Holz, R. C. Lysine biosynthesis in bacteria: a metallodesuccinylase as a potential antimicrobial target. *J. Biol. Inorg. Chem.* **2013**, *18* (2), 155−163.
(58) Hutton, C. A.; Perugini, M. A.; Gerrard, J. A. Inhibition of lysine biosynthesis: an evolving antibiotic strategy. *Mol. BioSyst.* **2007**, *3* (7), 458−465.
(59) Karita, M.; Etterbeek, M. L.; Forsyth, M. H.; Tummuru, M.; Blaser, M. J. Characterization of *Helicobacter pylori* dapE and construction of a conditionally lethal dapE mutant. *Infect. Immun.* **1997**, *65* (10), 4158−4164.
(60) Pavelka, M. S., Jr; Jacobs, W. R., Jr Biosynthesis of diaminopimelate, the precursor of lysine and a component of peptidoglycan, is an essential function of Mycobacterium smegmatis. *J. Bacteriol.* **1996**, *178* (22), 6496−6507.
(61) Reidl, C. T.; Heath, T. K.; Darwish, I.; Torrez, R. M.; Moore, M.; Gild, E.; Nocek, B. P.; Starus, A.; Holz, R. C.; Becker, D. P., Indoline-6-Sulfonamide Inhibitors of the Bacterial Enzyme DapE. *Antibiotics* **2020**, *9* (9), 595, DOI: 10.3390/antibiotics9090595
(62) Su, Y.-B.; Peng, B.; Li, H.; Cheng, Z.-X.; Zhang, T.-T.; Zhu, J.-X.; Li, D.; Li, M.-Y.; Ye, J.-Z.; Du, C.-C.; Zhang, S.; Zhao, X.-I.; Yang, M.-J.; Peng, X.-X. Pyruvate cycle increases aminoglycoside efficacy and provides respiratory energy in bacteria. *Proc. Natl. Acad. Sci. U. S. A.* **2018**, *115* (7), E1578−E1587.
(63) Irnov, I.; Wang, Z.; Jannetty, N. D.; Bustamante, J. A.; Rhee, K. Y.; Jacobs-Wagner, C. Crosstalk between the tricarboxylic acid cycle and peptidoglycan synthesis in Caulobacter crescentus through the homeostatic control of α-ketoglutarate. *PLoS Genet.* **2017**, *13* (8), No. e1006978.
(64) Thomas, V. C.; Kinkead, L. C.; Janssen, A.; Schaeffer, C. R.; Woods, K. M.; Lindgren, J. K.; Peaster, J. M.; Chaudhari, S. S.; Sadykov, M.; Jones, J.; AbdelGhani, S. M. M.; Zimmerman, M. C.; Bayles, K. W.; Somerville, G. A.; Fey, P. D. A Dysfunctional Tricarboxylic Acid Cycle Enhances Fitness of During β-Lactam Stress. *mBio* **2013**, *4* (4), No. e00437-13.
(65) Schutte, K. M.; Fisher, D. J.; Burdick, M. D.; Mehrad, B.; Mathers, A. J.; Mann, B. J.; Nakamoto, R. K.; Hughes, M. A. *Escherichia coli* Pyruvate Dehydrogenase Complex Is an Important Component of CXCL10-Mediated Antimicrobial Activity. *Infect. Immun.* **2016**, *84* (1), 320−328.
(66) Islam, M. M.; Tan, Y.; Hameed, H. M. A.; Liu, Z.; Chhotaray, C.; Liu, Y.; Lu, Z.; Cai, X.; Tang, Y.; Gao, Y.; Surineni, G.; Li, X.; Tan, S.; Guo, L.; Cai, X.; Yew, W. W.; Liu, J.; Zhong, N.; Zhang, T. Detection of novel mutations associated with independent resistance and cross-resistance to isoniazid and prothionamide in Mycobacterium tuberculosis clinical isolates. *Clin. Microbiol. Infect.* **2019**, *25* (8), 1041.e1−1041.e7.
(67) Dias, C. A.; Agnes, G.; Frazzon, A. P.; Kruger, F. D.; d'Azevedo, P. A.; Carvalho Mda, G.; Facklam, R. R.; Teixeira, L. M. Diversity of mutations in the atpC gene coding for the c Subunit of F0F1 ATPase in clinical isolates of Optochin-resistant *Streptococcus pneumoniae* from Brazil. *J. Clin. Microbiol.* **2007**, *45* (9), 3065−3067.
(68) Zasowski, E. J.; Rybak, J. M.; Rybak, M. J. The β-Lactams Strike Back: Ceftazidime-Avibactam. *Pharmacotherapy* **2015**, *35* (8), 755−770.
(69) Institute, T. C. a. L. S. *Performance Standards for Antimicrobial Susceptibility Testing*, 31 ed.; The Clinical and Laboratory Standards Institute: 950 West Valley Road, Suite 2500, Wayne, PA 19087−1898, United States, 2021.
(70) Bradford, P. A.; Huband, M. D.; Stone, G. G. A systematic approach to the selection of the appropriate avibactam concentration for use with ceftazidime in broth microdilution susceptibility testing. *Antimicrob. Agents Chemother.* **2018**, *62*, 7.
(71) Gika, H. G.; Theodoridis, G. A.; Wingate, J. E.; Wilson, I. D. Within-day reproducibility of an HPLC− MS-based method for metabonomic analysis: application to human urine. *J. Proteome Res.* **2007**, *6* (8), 3291−3303.
(72) Zhang, T.; Creek, D. J.; Barrett, M. P.; Blackburn, G.; Watson, D. G. Evaluation of coupling reversed phase, aqueous normal phase, and hydrophilic interaction liquid chromatography with Orbitrap mass spectrometry for metabolomic studies of human urine. *Anal. Chem.* **2012**, *84* (4), 1994−2001.
(73) Creek, D. J.; Jankevics, A.; Burgess, K. E.; Breitling, R.; Barrett, M. P. IDEOM: an Excel interface for analysis of LC-MS-based metabolomics data. *Bioinformatics* **2012**, *28* (7), 1048−1049.
(74) Scheltema, R. A.; Jankevics, A.; Jansen, R. C.; Swertz, M. A.; Breitling, R. PeakML/mzMatch: a file format, Java library, R library, and tool-chain for mass spectrometry data analysis. *Anal. Chem.* **2011**, *83* (7), 2786−2793.
(75) Smith, C. A.; Want, E. J.; O'Maille, G.; Abagyan, R.; Siuzdak, G. XCMS: processing mass spectrometry data for metabolite profiling using nonlinear peak alignment, matching, and identification. *Anal. Chem.* **2006**, *78* (3), 779−787.
(76) *Illumina, Nextera XT DNA library prep reference guide*; Illumina: San Diego, CA, 2019.
(77) Soneson, C.; Delorenzi, M. A comparison of methods for differential expression analysis of RNA-seq data. *BMC Bioinf.* **2013**, *14* (1), 91.

(78) Pirooznia, M.; Nagarajan, V.; Deng, Y. GeneVenn - A web application for comparing gene lists using Venn diagrams. *Bioinformation* **2007**, *1* (10), 420−422.
(79) Hadžija, O. A simple method for the quantitative determination of muramic acid. *Anal. Biochem.* **1974**, *60* (2), 512−517.

https://doi.org/10.1021/acsinfecdis.3c00264
ACS Infect. Dis. 2023, 9, 2409−2422